

Jet dynamics in black hole physics: acceleration during subparsec collimation*

Fernando de Felice [†]and Olindo Zanotti[‡]

August 31, 2018

Abstract

We study the processes of particle acceleration which take place in the field of a rotating black hole as part of a mechanism of formation of galactic jets within the first parsec from the central source, where gravitation is supposed to be dominant. We find the Lorentz factor that a stream of particles acquires as function of distance, when the orbital parameters vary slightly due to a local electromagnetic field or a pressure gradient.

1 Introduction

Jets emerging from active galactic nuclei are highly collimated structures (as revealed by radio maps) probably made of electron-positron plasma, which propagate in the intergalactic medium with relativistic velocities along most of their length (as implied by the detection of superluminal motion). It is then clear that one has to search for mechanisms which allow for both collimation and acceleration.

*Work partially supported by Ministero della Ricerca Scientifica e Tecnologica of Italy and by Gruppo Nazionale della Fisica Matematica del CNR

[†]Department of Physics G. Galilei, University of Padova, via Marzolo 8, I-35131 Padova Italy and INFN Sezione di Padova. E-mail: defelice@pd.infn.it

[‡]International School for Advanced Studies, SISSA, Trieste, Italy. E-mail: zanotti@sissa.it

On large scales (typically from parsec to kiloparsec) jets are currently studied within the framework of magnetohydrodynamics, to which we owe most of our knowledge about these structures. Through analytical and numerical models, we are now able to say something about electrodynamic confinement of axisymmetric flows, electromagnetic extraction of energy from rotating black holes through force-free magnetospheres and asymptotic poloidal velocities of hydromagnetic flows, to mention but a few. What is shared by most of these models is the need for plasma injection into a rapidly rotating magnetosphere from below.

Attention is then shifted to the subparsec scale, just outside the event horizon, where a primary acceleration mechanism must be at work. Recent developments (Sikora et al. 1996, [1]) have shown that such a mechanism cannot be powered by the radiation pressure of the accretion disk; this pressure, instead, causes the flow in the jet to decelerate by virtue of inverse Compton scattering with the plasma of the jet itself, with a maximum efficiency when the plasma's Lorentz factor has reached values higher than an equilibrium $\gamma_{eq} \sim 4$. That is to say, jets, accelerated in the subparsec region up to $\gamma_j \geq 5$, as revealed by VLBI measurements of superluminal motion in extragalactic radio sources, cannot avoid radiation drag. Notwithstanding this, we expect that at subparsec scale the gravitational field of a $10^8 \div 10^{11} M_\odot$ black hole should still play a major role in determining particles' motion; indeed the behaviour of individual particles is also that of the bulk of fluid elements in the guiding centre approximation. We then studied the combined effects of gravity and external physical perturbations. In de Felice and Carlotto (1997, [2]; hereafter Paper I) the collimating be-

haviour of geodesic orbits in the presence of a constrained variation of their energy and angular momentum was considered. The constraints are those which allow a particle, initially on a geodesic, to move on a nearby geodesic characterized by *slightly* varied parameters. In Paper I, this requirement was termed *geodesicity condition*. Following this line of thought, Karas and Dovicak (1997, [3]) have estimated the rate of change of the orbital parameters of individual particles and have integrated this rate over a power law distribution of particles' energy. Their results confirm our claim in Paper I that the approximation of geodesic motion in the presence of small perturbations, is appropriate for modelling the primary collimation of a jet.

Here we shall investigate whether the geodesicity conditions considered in Paper I, are compatible with the local Lorentz factor which is observed in galactic jets. Indeed we show that, provided there is a fine tuning between the stiffness of geodesic orbits and the effects of an external field, a large family of particle trajectories described by the Kerr metric not only collimate towards the axis of symmetry (see Paper I), but also accelerate, reaching values of the Lorentz factor γ , as measured by a local static observer, which are consistent with observations. Typically, we find $\gamma \leq 10$ at $1pc$ from the centre.

In Section 2 we summarize the general relativistic collimation effect discussed in Paper I, then in Section 3 we analyse the acceleration which test particles acquire under the condition of the mentioned collimation process. Behaviours of the local Lorentz factor γ are found as functions of distance from the central source for both the cases of Lorentz forces arising from a local electromagnetic field and from pressure gradients. Comparison with

observations must be handled with care: some comments on this problem are made in Section 4. Finally in Section 5, we pay particular attention to the limits imposed by the geodesicity conditions on the distance scale where the collimation mechanism is allowed to operate.

2 Geometrically induced collimation

In Paper I, de Felice and Carlotto studied the tendency of vortical geodesics, in a Kerr background geometry, to collimate towards the axis of symmetry under a constrained variation of the constants of the motion. Their claim was that such a property might be astrophysically relevant to allow for jets primary collimation very close to the central black hole. Here we shall summarize that reasoning.

Let the space-time be described by the Kerr metric in Boyer and Lindquist coordinates (t, r, θ, φ) :

$$\begin{aligned}
 ds^2 = & -\left(1 - \frac{2Mr}{\Sigma}\right)dt^2 - \frac{2\mathcal{A}}{\Sigma}\omega \sin^2 \theta dt d\varphi + \\
 & + \frac{\Sigma}{\Delta}dr^2 + \Sigma d\theta^2 + \frac{\mathcal{A}}{\Sigma} \sin^2 \theta d\varphi^2
 \end{aligned} \tag{1}$$

where

$$\Sigma = r^2 + a^2 \cos^2 \theta \tag{2}$$

$$\Delta = r^2 + a^2 - 2Mr \tag{3}$$

$$\mathcal{A} = (r^2 + a^2)^2 - a^2 \Delta \sin^2 \theta \tag{4}$$

$$\omega = \frac{2Mar}{\mathcal{A}} \tag{5}$$

M and a being respectively the total mass energy of the metric source and its specific angular momentum ($a = J/cM$), both expressed in geometrized

units ($c = G = 1$).

Attention is focused on a particular family of geodesics, namely the vortical ones. These curves are gravitationally unbound (open orbits) and are characterized by the following conditions ¹:

$$\Gamma > 0 \quad -a^2\Gamma \leq L \leq a^2\Gamma \quad L < l^2 \leq \frac{(L + a^2\Gamma)^2}{4a^2\Gamma} \quad (6)$$

In the absence of any external perturbation, l and $E = \sqrt{\Gamma + 1}$ are constants of the motion and express, respectively, the azimuthal angular momentum (in units of μc) and the total energy (in units of μc^2) of the particle along the orbit. L is the separation constant of the Hamilton-Jacobi equation in the Kerr metric and is related to the square of the total angular momentum of the particle (de Felice, 1980, [4]; de Felice and Preti 1998, [8]).

The permitted values of θ for the geodesic motion are confined (see figure 1) to the area below the functional curves:

$$l^2(\theta, L, \Gamma) = \sin^2 \theta (L + \Gamma a^2 \cos^2 \theta) \quad (7)$$

in the (l^2, θ) space (for any fixed pair of L and Γ), along which $\dot{\theta} = 0$. Given a constant value of l^2 in accordance with condition (6), vortical motion is found to be latitudinally confined within the range $[\theta_1, \theta_2]$ determined by the intersection of the straight line $l^2 = \text{const}$ with the functional curves (7). That is the reason why, vortical geodesics, which never cross the equatorial plane, are the most likely to leave the innermost part of an accretion disk surrounding a rotating black hole, through a spiralling motion.

Collimation is studied with respect to the opening angle of a particle beam centred on the axis ($\theta = 0$), taken for convenience to be equal to the

¹Vortical geodesics are also those with $\Gamma = l = L = 0$, but we shall not consider them here.

angle which makes l^2 vanish:

$$\cos^2 \theta_0 = -\frac{L}{\Gamma a^2}. \quad (8)$$

The cornerstone of the reasoning is to presume that, in the innermost region of the field, relation (8) continues to hold even under a slow variation of the parameters Γ and L induced by some sort of external perturbation to the plain geodesic motion.

In order to prevent the geodesic character of the motion being lost because of the perturbations, we will impose “geodesicity conditions” with the effect of forcing each particle on a vortical geodesic to drift onto a nearby geodesic of the same type.

In this case, differentiation of (8) with respect to the proper time τ along the trajectories, leads to the basic equation of jet dynamics:

$$-2L \tan \theta_0 \frac{d\theta_0}{d\tau} = a^2 \cos^2 \theta_0 \frac{d\Gamma}{d\tau} + \frac{dL}{d\tau}. \quad (9)$$

The existence of vortical trajectories in the space-time of a Kerr black hole, is a general relativistic effect which stems from the rotational properties of the metric, (see also O’Neil (1995) [9]). While the vortical character of the orbits with parameters as in (6), is a natural consequence of gravitational dragging, the trend to axial collimation, as a result of a small perturbation, was quite unexpected. This effect is entirely due to the first term on the right-hand-side of equation (9) which contains the rotational parameter a . Evidently, when $a = 0$, there are no vortical orbits and no axial collimation; this implies that sufficiently small values of a would make the effect negligibly small. However, if we consider, as source of the orbital perturbations,

physical fields that share the same symmetries as the metric source, as expected very near to the black hole, the collimation follows laws which do not depend explicitly on a (see equations (10) to (12) below), suggesting a kind of contradiction. Indeed, the dependence on a comes implicitly through the very form of the equations of motion and the equations of the perturbing fields. Parameter a fixes, from relations (6), the range of the permitted vortical orbits; when a becomes small, this range shrinks (see figure 1), so what decreases is not the *amount* of collimation, but the *number* of orbits which are involved. For this reason, this general relativistic effect may not be negligible at astrophysical scales.

The explicit form of the variations $(d\Gamma/d\tau)$ and $(dL/d\tau)$ of the orbital parameters, depends on the nature of the perturbation we consider. As shown in Paper I, in the presence of a local electromagnetic field or of a pressure gradient, which are the two perturbations we are going to deal with, relations exist which link the coordinate θ to the energy parameter Γ . In case of energy gain ($\frac{d\Gamma}{d\tau} > 0$), such relations give rise to collimation laws, which we now recall:

- Case of poloidal electromagnetic field (see section 3.1):

– cospiralling $\theta = \text{const.}$ orbits:

$$\sin \theta = \sin \theta_i \left[\frac{\sqrt{1 + 1/\Gamma} + 1 + 1/(2\Gamma)}{\sqrt{1 + 1/\Gamma_i} + 1 + 1/(2\Gamma_i)} \right]^{1/4} \quad (10)$$

– counterspiralling $\theta = \text{const.}$ orbits:

$$\sin \theta = \sin \theta_i \left[\frac{\Gamma_i(\sqrt{\Gamma_i^2 + \Gamma_i} + 1/2 + \Gamma_i)}{\Gamma(\sqrt{\Gamma^2 + \Gamma} + 1/2 + \Gamma)} \right]^{1/4} \quad (11)$$

- Case of pressure gradients (see section 3.2):

– Either case of $\theta = \text{const.}$ orbits:

$$\sin \theta = \sin \theta_i \left[\frac{\Gamma_i(\Gamma + 1)}{\Gamma(\Gamma_i + 1)} \right]^{1/4} \quad (12)$$

where θ_i and Γ_i are the initial values. In figure 2 and 3 we show the collimating behaviour of (10), (11) and (12) under the influence of the corresponding external perturbation which causes an increase of particle's energy. We have chosen as initial values, $\Gamma_i = 0.1$ at $\theta_i = \pi/4$.

Distinction has been made between co-rotating (with the metric source) and counter-rotating orbits, collimation being stronger for the latter ². Let us underline the physical meaning of these relations: geometry induced collimation, in the presence of an electromagnetic field or a pressure gradient, occurs mainly when particles, on initially vortical geodesics, increase their energy with respect to infinity. However this is not the same as saying that they are locally accelerating, as we are going to see.

3 Test particle acceleration

Relations (10) - (11) - (12) presuppose a knowledge of how Γ varies along the perturbed geodesic under the two kinds of external perturbations we are here considering. In this way, besides describing the collimation of the vortical geodesics, we will also deduce the behaviour of the local Lorentz factor γ of the particles which leave the neighbourhood of the rotating black hole.

²Curves of figure 2 correct figure 4 of Paper I where they have been erroneously crossed. In that figure the two curves had to be considered independently and not to be compared.

Let us introduce a field of local static observers defined by a four-velocity:

$$\tilde{u} = (-g_{00})^{-1/2} \partial_t = e^\psi \partial_t \quad (13)$$

and let \tilde{k} be the particle four-velocity. The relation between the total particle energy E , as measured at asymptotic distances, and the fundamental astrophysical quantity γ locally measured by the observer \tilde{u} , is then given by:

$$\gamma = -(\tilde{u}|\tilde{k}) = -e^\psi (\partial_t|\tilde{k}) = e^\psi E \quad (14)$$

that is:

$$\gamma = \sqrt{\frac{\Gamma + 1}{1 - \frac{2Mr}{r^2 + a^2 \cos^2 \theta}}} \quad (15)$$

where M , as stated, is the mass of the black hole.

For the sake of comparison, let us first consider the behaviour of γ for a particle in strictly geodesic motion, namely in the absence of external perturbations.

Suppose the particle is moving outwardly on a geodesic with $\theta = \text{const} = 0.1$ rad, arriving at infinity with $\gamma_\infty = e^{\psi(\infty)} E = E = 1.1$, starting from $\bar{r}_i = r_i/M = 1.5$ with $\gamma_i = 1.1 e^{\psi(\bar{r}_i, \theta_i)} = 4.07$ ³. As we can see from fig 4, the particle is progressively slowed down as seen by a local static observer as it moves on its outwardly path. Such a trend reflects the attractive character of gravity, according to intuition. We have chosen $\bar{a} = a/M = 0.9981$.

In what follows we shall analyse the behaviour of γ in a stream of particles under the influence of an electromagnetic field and a pressure gradient, constrained however by the geodesicity conditions which guarantee the simultaneous occurrence of collimation.

³ Being $1M_\odot = 2.2 \cdot 10^3 m$ in geometrized units, $\bar{r}_i = 1.5$ corresponds to a distance from a $10^8 M_\odot$ black hole of $r_i = \bar{r}_i \cdot M = 3.3 \cdot 10^{11} m \sim 10^{-5} pc$.

3.1 Effects of the electromagnetic field

The electromagnetic field we consider arises locally from the potential:

$$A = -\frac{Qr}{\Sigma}(dt - a \sin^2 \theta d\varphi) \quad (16)$$

where Q is the total electric charge.

A charged particle of rest mass μ and charge q will deviate from geodesic motion by the term (neglecting radiation reaction):

$$\tilde{k}^r \nabla_r \tilde{k}_i = \frac{q}{\mu} F_{ij} \tilde{k}^j \quad (17)$$

where $F_{ij} = 2\partial_{[i}A_{j]}$ and \tilde{k} is, as stated, the 4-velocity of the particle. Since $\tilde{k}_0 = -E$, we easily deduce:

$$-\frac{dE}{d\tau} = \frac{qQ}{\mu\Sigma^2} \left[(a^2 \cos^2 \theta - r^2) \frac{dr}{d\tau} + ra^2 \sin 2\theta \frac{d\theta}{d\tau} \right] \quad (18)$$

which tells us how E varies along the perturbed geodesic. Since the variation of E is much more sensitive to the variation of the coordinate r than to θ , decreasing as $(M/r)^2$ in the first case and as $(M/r)^4$ in the latter, we can take as full variation of E the following:

$$\frac{\partial E}{\partial r} = \frac{qQ}{\mu\Sigma^2} (r^2 - a^2 \cos^2 \theta) \quad (19)$$

Recalling that $E = \sqrt{\Gamma + 1}$ and using normalized quantities, relation (19) can be written as:

$$\frac{\partial \Gamma}{\partial \bar{r}} = 2\bar{C} \frac{\bar{r}^2 - \bar{a}^2 \cos^2 \theta}{(\bar{r}^2 + \bar{a}^2 \cos^2 \theta)^2} \sqrt{\Gamma + 1} \quad (20)$$

where we have put $\bar{C} = \frac{qQ}{\mu M}$.

This is the partial differential equation we were looking for. It can be coupled to the laws of collimation (10) and (11), providing a system in

the unknowns $\Gamma(\bar{r})$ and $\theta(\Gamma(\bar{r}))$. This allows us to reduce (20) from the form $\partial_{\bar{r}}\Gamma = f(\Gamma, \bar{r}, \bar{a} \cos \theta)$ to the form $\partial_{\bar{r}}\Gamma = g(\Gamma, \bar{r})$, exploiting the laws of collimation we have already found. The new partial differential equation can be numerically solved for $\Gamma(\bar{r})$, telling us how Γ varies along the perturbed geodesic as a function of distance. On the other hand, knowledge of $\Gamma(\bar{r})$ allows us to find the value of θ as a function of r . Getting the Lorentz factor $\gamma = \gamma(\bar{r})$ would be the last step, through relation (15) with the laws of collimation to be used again.

All seems to be quite smooth, except for the presence of parameter \bar{C} : in Paper I it was shown that having a magnetic field $B \sim 10^{-3}G$ at the distance of $1pc$ from a $10^8 M_{\odot}$ black hole along the axis, implies $Q \sim 2.3 \cdot 10^{11}m$ in geometrized units, so that $Q/M \sim 1$. Consequently, \bar{C} is mainly the ratio q/μ , which depends critically on the ionization degree.

Since we are interested in the bulk motion of the material, rather than the motion of individual particles, we can accept the guiding centre approximation and look at our particle as a small cloud of hydrogen, say, whose specific charge we need to estimate. This requires taking into account the effects of photoionization due to the radiation field of the central source, the degree of recombination, the optical depth within the cloudlet itself and the gravitational redshift of the ionizing radiation. But first of all, we ought to know what kind of conditions on ratio q/μ comes from the geodesicity condition, so essential to our discussion. As stated in Paper I, the geodesic character of the motion can be approximately saved if orbital parameters vary slowly in time, geodesicity being better preserved where gravity dominates. This led the authors to evaluate the changes of energy of an orbit

that deviates from a geodesic under the effects of an electromagnetic field, written in terms of coordinates proper values variations (relations (41) of Paper I) as:

$$\begin{aligned}
\delta E|_{\theta=const} &= \frac{\partial E}{\partial r} \delta r \\
&= \frac{q}{\mu} \frac{Q}{M} M \frac{r^2 - a^2 \cos^2 \theta}{(r^2 + a^2 \cos^2 \theta)^2} \delta r \\
&= \frac{q}{\mu} \frac{Q}{M} \left(\frac{M}{r}\right)^2 \left(\frac{\Delta}{\Sigma}\right)^{1/2} \frac{1 - (a^2/r^2) \cos^2 \theta}{[1 + (a^2/r^2) \cos^2 \theta]^2} \delta\left(\frac{l_r}{M}\right) \quad (21)
\end{aligned}$$

where $\delta l_r = (g_{rr})^{1/2} \delta r$ is the proper-radial length as it would be measured by the particle itself. Since a variation of l_r goes on with dynamical time while a variation of the parameter E goes with the perturbation time, the geodesicity conditions require that $\delta E < \delta l_r$.

More precisely, what we ask is that the timescale of a significant variation of the physical parameters, τ_{var} , be longer than the dynamical time associated with a geodesic trajectory, τ_{dyn} . Just for an order of magnitude estimate, let us take, as a significant dynamical time, the proper time a particle takes to reach the $r = 0$ disk from the outer horizon on a parabolic trajectory, as was shown in Paper I:

$$\tau_{dyn} \sim \frac{2M}{3} \left[1 + \sqrt{1 - \left(\frac{a}{M}\right)^2} \right] \sim \frac{2M}{3} \quad (22)$$

On the other hand:

$$\tau_{var} \sim \left(E / \frac{dE}{d\tau} \right) \sim \frac{E}{\frac{qQ}{\mu\Sigma^2} (r^2 - a^2 \cos^2 \theta) \frac{dr}{d\tau}} \quad (23)$$

If we now recover from (A1) of Paper I the r component of the four-vector \tilde{k} tangent to a $\theta = 0$ geodesic in which we choose, for simplicity, $\Gamma \simeq 1$:

$$k^r = \left(\frac{r^2 + a^2 + 2Mr}{r^2 + a^2} \right)^{1/2} \quad (24)$$

we get:

$$\tau_{var} \sim \frac{\sqrt{2}(r^2 + a^2)^{5/2}}{\frac{q}{\mu}Q(r^2 - a^2)(r^2 + a^2 + 2Mr)^{1/2}} \quad (25)$$

Therefore the geodesicity condition translated into timescale language requires that:

$$\frac{q}{\mu} < \frac{3}{2}\sqrt{2}\frac{(\bar{r}^2 + \bar{a}^2)^{5/2}}{(\bar{r}^2 - \bar{a}^2)(\bar{r}^2 + \bar{a}^2 + 2\bar{r})^{1/2}} \equiv \bar{C}_{ms} \quad (26)$$

This is an explicit, though crude, expression of the geodesicity condition in the presence of the particular electromagnetic field we have considered. It can be either considered as a condition on the ratio q/μ if we fix the distance r from the source, or as a condition on the distance scale if we can fix the ionization. Taking as mentioned $Q/M \sim 1$ and $a/M \sim 0.9981$, (26) tells us that q/μ must be of the order ≤ 10 at short distances from the centre ($r = 2M$), while it can increase outwardly up to $q/\mu \leq 10^{10}$ at $r \sim 10^5 M \sim 1pc$.

The astrophysical implications of these requirements have been discussed in Paper I, therefore we shall here derive the behaviour of $\gamma(r)$ with the assumption that the conditions on q/μ are satisfied⁴. That is, we are now in a position to integrate equation (20) and get the behaviour of $\gamma(\bar{r})$ through relation (15), provided we take \bar{C} values in accordance with condition (26).

To a first approach, we will fix \bar{C} to some constant (and low) value, so as to reproduce the behaviour of an approximately neutral plasma. Secondly, we will consider \bar{C} linearly rising from the centre towards the outer regions, so as to reproduce the behaviour of increasingly ionized plasma, as it could

⁴Since the order of magnitude of the ratio q/μ for an electron is, in geometrized units, $q/\mu \sim 10^{21}$, we can deduce that for the geodesicity condition to be satisfied, we ought to deal with cloudlets which are almost neutral near the horizon, and increase their ionization as we move outwards. Evidently, we shall refer to q/μ as the average degree of ionization in a volume element, rather than to the specific charge carried by a single particle.

be under the effect of a ionizing flux of radiation. That such a trend satisfies condition (26) can be appreciated in figure 5, where it is compared with the plot of \bar{C}_{ms} .

Figures (6) to (9) contain the results of the first approach. They show the $\gamma(\bar{r})$ profiles obtained through the mechanism just outlined, where we have chosen $\bar{C} = 2.5, 5, 10$ on a distance scale ranging from $\bar{r}_i = 2.3$ to $\bar{r} = 100$, that is to say from almost outside the event horizon to $r \sim 10^{-3}$ pc from the centre. Each figure shows two curves, one for co-spiralling orbits (solid line), and the other for counter-spiralling ones (dashed line).

Figures (10) and (11) contain the results of the second approach. They show the γ profiles obtained with linearly rising \bar{C} values, that is to say with $\bar{C} \sim \beta\bar{r}$, with $\beta = 0.8$ and $\beta = 1.1$. The distance scale has been enlarged up to the first parsec from the central source. Only one curve has been drawn in this case, because the profiles for co-rotating and counter-rotating orbits superimpose at such distances.

The following aspects can be underlined:

- we are facing an acceleration mechanism, which increases both Γ and γ up to asymptotic adjustments in dependence of parameter \bar{C} . We typically find $\gamma \sim 2 \div 4$ at $10^{-3}pc$ from the centre, and $\gamma \sim 10$ at the distance of $1pc$. For constant values of \bar{C} , slightly higher Lorentz factors are reached on co-rotating orbits with respect to counter-rotating ones; the difference disappears on larger scales when \bar{C} is supposed to rise linearly.
- we can appreciate the distinction between parameter Γ , which is linked to energy E and which is always raising, and the Lorentz factor γ ,

which is the quantity measured by the local observer. Contrary to Γ , γ shows a rapid decay within the first $r \sim 10M$ from the centre (see figure 7), where the effects of gravity are supposed to overwhelm those of the electromagnetic field. As a matter of fact, γ profiles in this inner region can be almost superimposed on those we found for the geodesic motion, proving the stiffness of geodesic orbits very near the central black hole.

- In our calculations we have chosen an initial value of $\Gamma_i = 0.1$ at $\bar{r}_i = 2.3$ and $\theta_i = \pi/4$, meaning an initial value of $\gamma_i \sim 2.3$. What can power particles do to such a relatively high value of the Lorentz factor just outside the event horizon? The question is still open: some version of the Penrose mechanism has been proposed (Reva K. 1995, [5]).
- we should pay attention to the fact that the mechanism we have just explored coexists with radiation pressure effects. As we have mentioned in the introduction, inverse Compton interaction of the plasma in the jet with the radiation field produces a net deceleration, which always arises when the Lorentz factor of the bulk motion exceeds an equilibrium regime given by $\gamma_{eq} \sim 4$, depending on the radiation field distribution one adopts. Though in this Paper we have not considered radiation field as a possible physical perturbation, we can argue, looking at our γ profiles, that radiation drag will not occur within $10^{-3}pc$ from the centre, where γ does not exceed the value of 5. Far from the black hole, at $1pc$ from it, we find $\gamma \sim 10$, so there might be a perceivable effect of radiation drag tending to lower γ to its equilibrium

value. But far from the black hole, according to Sikora et al. (1996), such an effect decreases in importance.

3.2 Effects of the pressure gradient

Let us now consider the effects on the geodesic motion of the perturbation represented by pressure gradients, which probably characterize the inner parts of an active galactic nucleus:

$$p \sim \rho^\alpha \quad (27)$$

$$\rho \sim r^{-n} \quad (28)$$

with $1 < n < 3$, as suggested by several polytropic models.

These pressures and densities are assumed to be those of a perfect fluid, whose elements approximate the behaviour of the emerging particles. The relativistic Euler equation leads to a variation of the energy of each fluid element along the perturbed trajectory, given by:

$$\frac{dE}{d\tau} = -\frac{E}{p + \rho} \frac{dp}{d\tau} \quad (29)$$

For the same reasons we appealed to in the electromagnetic field perturbation case, (29) transforms into:

$$\partial_r \Gamma = -\frac{2(\Gamma + 1)}{p + \rho} \partial_r p \quad (30)$$

which is analogous to equation (19). It can be further developed if we take $p = A\rho^\alpha$ and $\rho = Br^{-n}$, without specific knowledge of the constants A and B :

$$\partial_{\bar{r}} \Gamma = \frac{2n\alpha \bar{D}(\Gamma + 1) \bar{r}^{n(1-\alpha)-1}}{1 + \mathcal{D} \bar{r}^{n(1-\alpha)}} \quad (31)$$

where we have put $\bar{\mathcal{D}} = \frac{AB^{\alpha-1}}{M^{n(\alpha-1)}}$.

Once again we need to evaluate energy changes on a $\theta = \text{const}$ perturbed geodesic, in order to see what kind of geodesicity condition we have to account for. From Paper I we deduce:

$$\delta E|_{\theta=\text{const}} \leq E \left| \frac{r}{\rho} \frac{\partial p}{\partial r} \right| \left(\frac{M}{r} \right) \left(\frac{\Delta}{\Sigma} \right)^{1/2} \delta \left(\frac{l_r}{M} \right) \quad (32)$$

with the inferred requirement that, at least:

$$\left| \frac{r}{\rho} \frac{\partial p}{\partial r} \right| < 1; \quad (33)$$

such a condition is equivalent to the requirement that the sound speed in the comoving frame of the fluid is non-relativistic:

$$v_s < \frac{1}{\sqrt{n}} \quad (34)$$

The last step is now to choose realistic values for α and n . Theoretical arguments combined to semiempirical estimates of pressure based on VLBI measurements (see Begelman 1984, [6]) seem to converge on $\alpha = 2$, $n = 2$ as the best choice⁵. Therefore, the differential equation to integrate is, from (31):

$$\partial_{\bar{r}} \Gamma = \frac{8\bar{\mathcal{D}}(\Gamma + 1)}{\bar{r}^3 + \bar{\mathcal{D}}\bar{r}} \quad (35)$$

with the associated geodesicity condition that, from (34), is:

$$v_s < \frac{1}{\sqrt{2}} \quad (36)$$

This latter condition implies a lower limit to the distance scale where the mechanism can operate. In order to see this, let us write down the behaviour

⁵ α and n are not independent: for polytropic gases of the kind we are discussing we know that $n = \alpha/(\alpha - 1)$.

of v_s upon r as it results if we remember the definition $v_s^2 = \partial p / \partial \rho$ with our expressions for pressure and density:

$$v_s^2 \sim \alpha \bar{\mathcal{D}} \bar{r}^{-n(\alpha-1)} \quad (37)$$

and, with our choices for n and α :

$$v_s \sim \sqrt{2\bar{\mathcal{D}}} \bar{r}^{-1} \quad (38)$$

Now, given a value of $\bar{\mathcal{D}}$, (38) yields the behaviour of v_s , which must satisfy (36). Hence there exists a lower limit in the distance scale, given by $\bar{r}_{lb} = 2\sqrt{\bar{\mathcal{D}}}$.

We have numerically solved equation (35) using low values of $\bar{\mathcal{D}}$. The Lorentz factor γ comes from (15), with the appropriate law of collimation offered by (12). Figures (12), (13) and (14) show the results of our calculations: the distance scale extends from a point $\bar{r}_i = 2\sqrt{\bar{\mathcal{D}}}$ (in all cases near the event horizon) to $\sim 10^{-2}$ parsec from the centre. As we can see, the Lorentz factor shows a maximum at distances an order of magnitude farther than the event horizon from the centre, depending on parameter $\bar{\mathcal{D}}$. At large distances, γ tends to decrease, adjusting itself to a constant value. The mechanism seems to be most efficient in the very central regions of the field.

4 Comparison with observations

Some facts make it difficult to speak of an effective comparison with observations:

- what can be observed and measured, through the analysis of VLBI maps, is the proper motion of a radio pattern along the jet. Knowledge

of the redshift z of the source, combined with a hypothesis on the cosmological parameters q_0 and H_0 , allow us to derive the apparent velocity β_{app} at which the radio components are seen to be moving. Superluminal motion is detected over a wide distance range, starting from $10^{-2}pc$ from the core, up to $10^2 \div 10^3pc$ far away from it.

The Lorentz factor corresponding to the superluminal motion that is usually observed with the above mentioned method is assumed to coincide with the Lorentz factor of the plasma bulk motion along the jet, responsible for the Doppler boosting of the radiation.

- in such a manner, statistical analysis carried out on a sample of sources, for which superluminal motion has been detected, yield the following mean values of the Lorentz factor (taken from data of Ghisellini et al., 1993, [7]) :

Sources	γ
BL Lac	10.47 ± 1.35
CDQs	16.98 ± 1.25
LDQs	14.45 ± 1.38

Table 1: Mean values of the Lorentz factor for the sample of sources in the paper of Ghisellini et al. CDQs and LDQs refer respectively to core dominated quasars and lobe dominated quasars.

What these data do not tell us is the distance from the source where the Lorentz factor has been measured, while our γ values refer to distances within the first parsec from the centre.

- our γ profiles have been found in the single-particle approach for the

case of the electromagnetic field perturbation, and in the hydrodynamical approach for the case of the pressure gradient perturbation. This guiding centre approximation is the first step towards a full magnetohydrodynamical treatment.

- Lorentz factors γ derived from observations are found within the framework of special relativity, assuming relativistic motion of the outgoing plasma along a direction making an angle φ with respect to the line of sight. Therefore, we have stressed the importance of having introduced a local observer, because around him special relativity holds, so that what he measures is approximately what we measure from earth, apart from negligible problems due to the choice of a particular local observer (we found it useful to choose a local static observer).

What is more, a direct comparison with observations is impossible unless we take into account the major role of large scale magnetic fields in extracting rotational energy from the black hole. Instead, what can be reasonably said is that the mechanisms we have proposed serve as primary acceleration mechanisms able to inject the plasma into the magnetosphere with values of the Lorentz factor γ around $5 \div 10$.

5 The distance scale

The most important restrictions to the efficiency of the acceleration mechanisms we have just outlined are represented by the geodesicity conditions, which turn out to establish conditions on the ionization degree, combined with conditions on the distance scale where the mechanisms can operate.

There does not seem to be any upper limit to the distance scale for the mechanisms we have developed, while there is a potential lower limit for both types of perturbation we have considered. Let us justify these statements starting from the electromagnetic field perturbation.

If we come back to figure 5 we can infer the existence of a lower limit to the distance scale: since the curve describes the maximum degree of ionization allowed, a high constant value of q/μ would violate the geodesicity condition at short distances. The higher the value of q/μ , the farther the lower limit is from the centre. That is the reason why in our calculations we have chosen low constant values for parameter \bar{C} . Similarly, a linearly rising degree of ionization satisfies the geodesicity condition all along the distance scale, as the figure shows.

On the other hand, it is the very nature of the electromagnetic potential to prevent the existence of an upper limit to the distance scale. In fact, both A_t and A_φ of potential (16) vanish at infinity. This suggests that the effects of the electromagnetic field would vanish as we moved outwardly⁶ and we have found that the behaviour of Γ confirms this conclusion: Γ adjusts itself to a constant value far from the centre, as would be the case of a plain geodesic motion ($\delta E \rightarrow 0$). Only the case of a degree of ionization intersecting the limiting curve of figure (5) from below would violate the geodesicity condition far from the centre, giving rise to an upper limit of the

⁶With a different choice of the electromagnetic field, such as that cited by Karas & Dovciak:

$$\begin{aligned} A_t &= \beta a [r\Sigma^{-1}(1 + \cos^2 \theta) - 1] \\ A_\varphi &= \beta \sin^2 \theta [1/2(r^2 + a^2) - a^2 r \Sigma^{-1}(1 + \cos^2 \theta)] \end{aligned}$$

$\beta \simeq 5 \cdot 10^{-8} (B/10^4 \text{ Gauss})(M/10^8 M_\odot) \simeq 10^{-8}$, the situation would have been different and we would have probably found an upper bound too.

distance scale, but that seems to be quite unphysical.

Now let us turn to the pressure gradient case. We have already shown the existence of a lower limit in the distance scale, depending on the value of \bar{D} : the higher the value of \bar{D} , the farther the lower limit from the centre. No upper limit can be found either: that is physically suggested by the fact that pressure gradients vanish at infinity as $\partial p/\partial r \sim r^{-5}$ so v_s decreases monotonically in such a way that condition (34) is always satisfied far from the black hole.

In this sense, the acceleration mechanisms we have proposed need particular care near the centre, where we have to hinder the effects of extreme physical conditions, while they die a natural death far from the black hole. Therefore, there is no point in extending the integration beyond the first parsec from the centre, since neither the local electromagnetic field, nor the pressure gradients have any more appreciable effect on the motion at those distances.

6 Conclusions

Radio components in jets emerging from active galactic nuclei are found to undergo superluminal expansion both near the core, at $10^{-2}pc$ from the centre, and far away from it, at $10^2 - 10^3pc$. Let us just cite 3C 273, that shows components in superluminal motion at $\sim 50pc$ from the core (S.C. Unwin 1989, [10]); 3C 345, studied at $22GHz$, which shows superluminal expansion on the parsec scale ($5 - 25pc$ from the core), and 0836+71, which shows superluminal motion at $\sim 220pc$ from the centre.

Therefore, observations suggest that jets are born with high Lorentz

factors. In Paper I we indicated that these structures emerge already collimated in the inner region of an AGN, instead of being collimated by large scale magnetic fields. In this Paper we have tried to complete the picture, testing the capability of a properly perturbed gravitational field to produce relatively large local Lorentz factors of escaping particles within the first parsec from the centre.

We are now in a position to talk of collimation after acceleration, which would occur in the inner region of an AGN, where the effects of the black hole space time geometry mix with those of external perturbations, namely a local electromagnetic field and pressure gradients. Important restrictions on the ionization degree of a testing cloudlet have been introduced, in order to preserve the geodesic character of the motion; specifically, we have found that a degree of ionization which rises linearly with distance from the core is compatible with quasi-geodesicity.

The nature of the interaction between the charged cloudlets and the electromagnetic field has been studied limitedly to the Lorentz forces which arise: more subtle effects such as Compton losses have been neglected. This idealized picture can be justified if we consider the order of magnitude of the competing forces, namely gravoinertial against Lorentz ones. As a consequence, the proposed mechanisms show most of their efficiency within the first parsec from the centre, producing values of the local Lorentz factor γ in the range $5 \div 10$, depending on the parameters introduced. We claim that the nozzle appealed to by some hydrodynamical models could be a point in the region between $10^2 \div 10^3 r_g$ from the core, where we find values of the Lorentz factor between $4 \div 8$ for the two cases of perturbation studied.

It is to the distance scale to which we refer when we define the above developed acceleration mechanisms as primary acceleration mechanisms, and we can but confirm the need to look for different physical processes to account for the velocity regime of jets, starting from the subparsec region and ending in the external radio lobes.

Acknowledgments Thanks are due to Prof. Mary Evans Prosperi for correcting the English text.

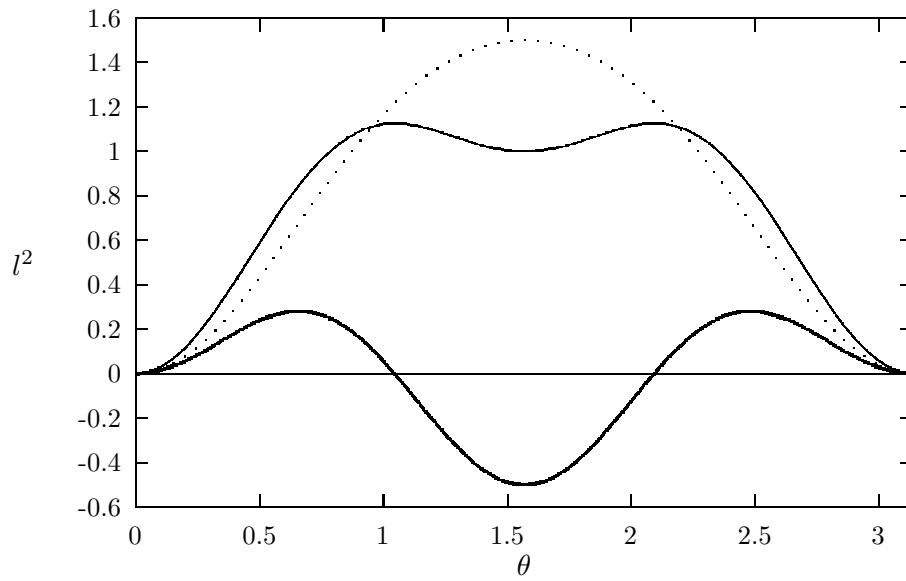


Figure 1: Plots of the functions $l^2 = l^2(\theta, \Gamma, L)$, when $\Gamma > 0$.

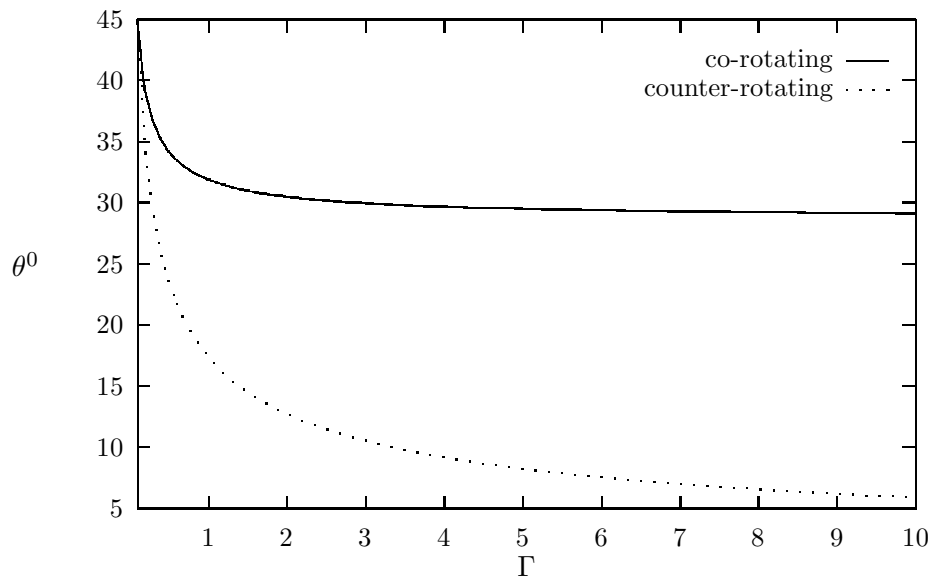


Figure 2: Behaviour of the angle of collimation for corotating and counter-rotating outgoing particles which increase their energy with respect to infinity, under the influence of a poloidal magnetic field. $\Gamma_i = 0.1$, $\theta_i = \pi/4$.

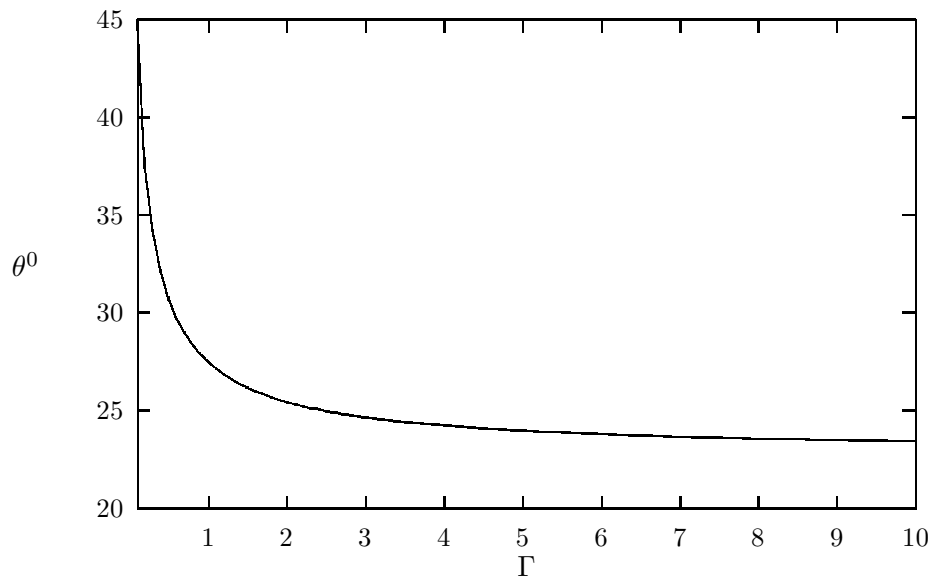


Figure 3: Behaviour of the angle of collimation for outgoing particles (corotating and counter rotating) which increase their energy with respect to infinity, under the influence of a pressure gradient. $\Gamma_i = 0.1$, $\theta_i = \pi/4$.

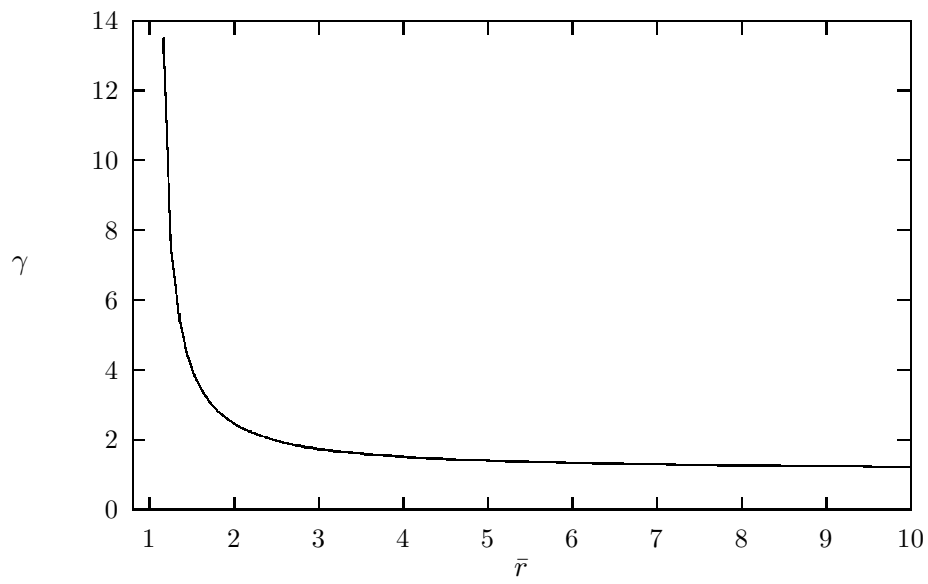


Figure 4: Lorentz factor for a particle on a plain geodesic motion. $\theta = 0.1 \text{ rad}$, $E = 1.1$

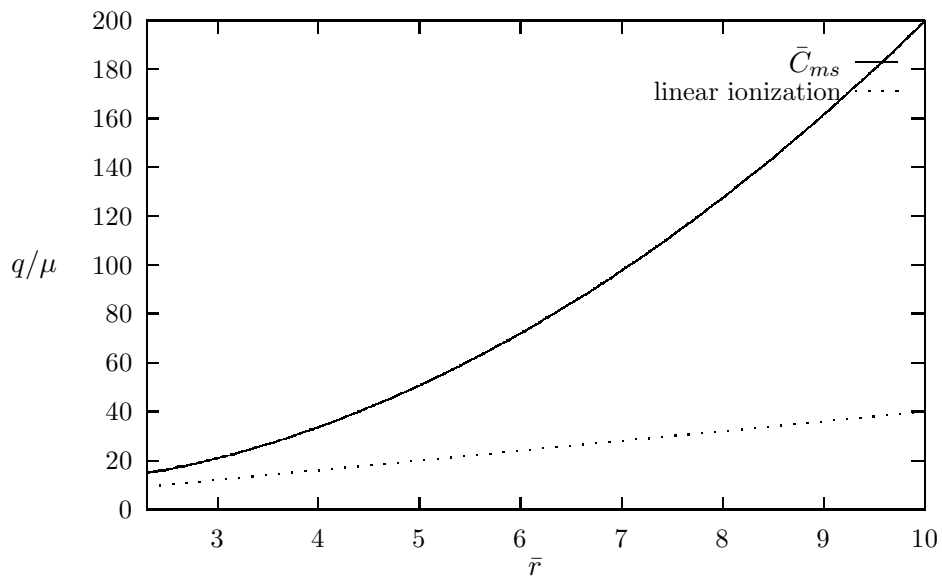


Figure 5: The figure shows how a straight line representing a linearly rising ionization ($q/\mu \simeq 4\bar{r}$) is always below the curve \bar{C}_{ms} in equation (26) which limits the validity of geodesicity condition.

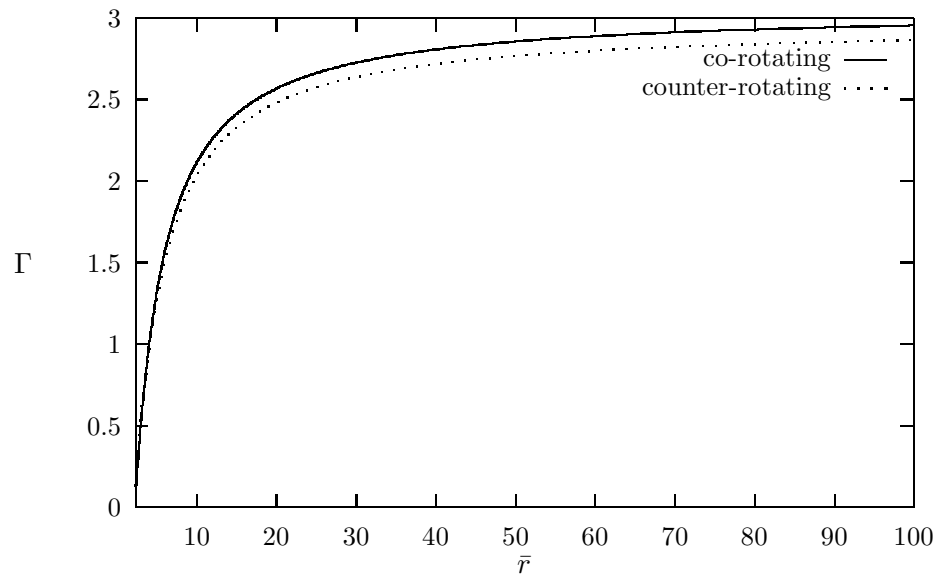


Figure 6: Behaviour of Γ upon distance for co-rotating and counter-rotating orbits under the effect of the electromagnetic field. $\bar{\mathcal{C}} = 2.5$, $\Gamma_i = 0.1$, $\bar{r}_i = 2.3$.

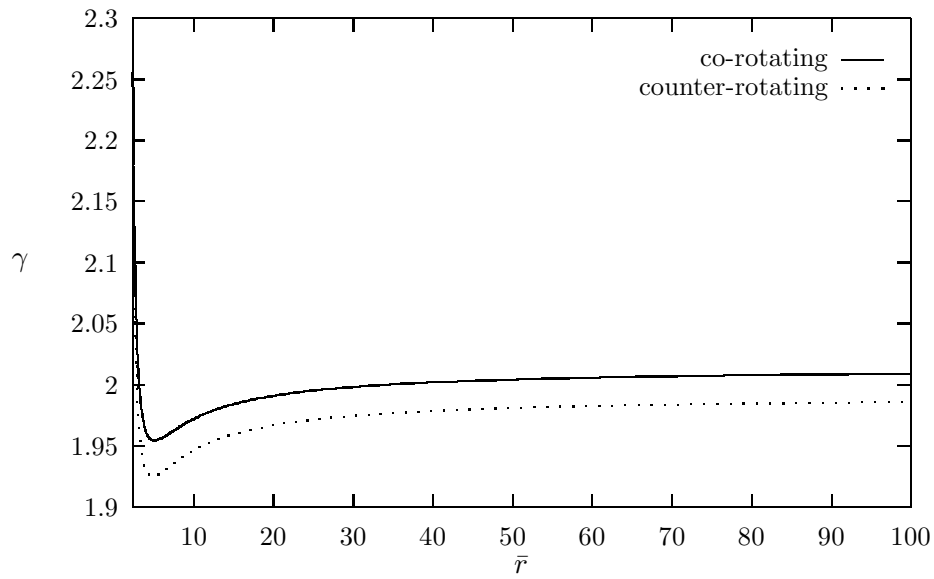


Figure 7: Behaviour of the Lorentz factor γ corresponding to the values of Γ represented in figure 6.

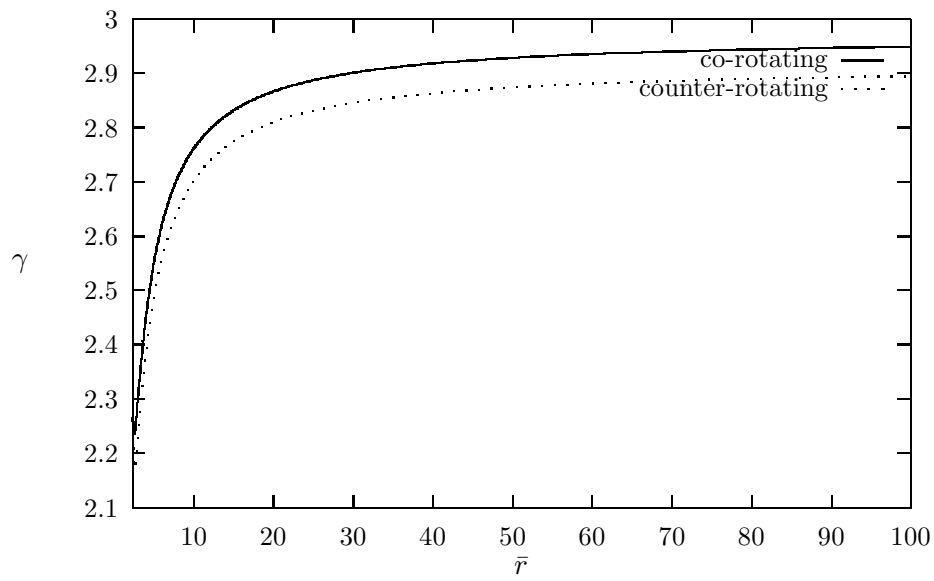


Figure 8: Behaviour of the Lorentz factor γ upon distance for co-rotating and counter-rotating orbits under the effect of the electromagnetic field. $\bar{C} = 5$, $\Gamma_i = 0.1$, $\bar{r}_i = 2.3$.

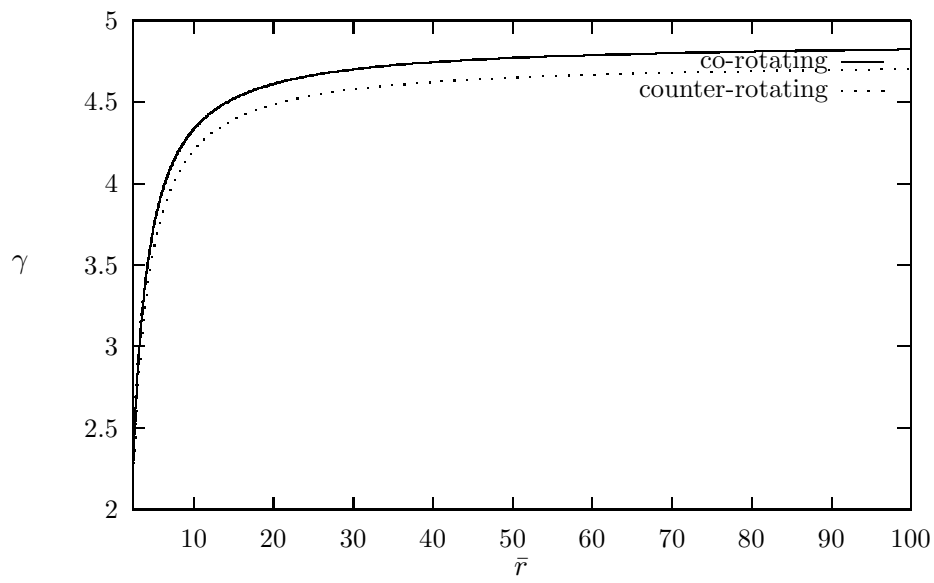


Figure 9: Behaviour of the Lorentz factor γ upon distance for co-rotating and counter-rotating orbits under the effect of the electromagnetic field. $\bar{C} = 10$, $\Gamma_i = 0.1$, $\bar{r}_i = 2.3$.

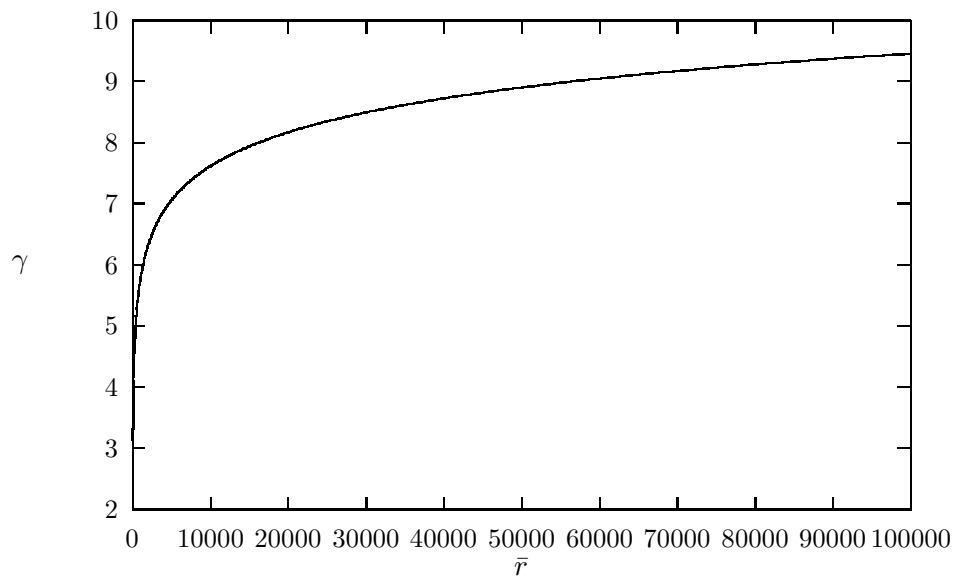


Figure 10: Behaviour of the Lorentz factor γ for co-rotating and counter-rotating orbits with a linearly rising degree of ionization: $\bar{C} = 0.8\bar{r}$; distance scale enlarged to the first parsec from the centre .

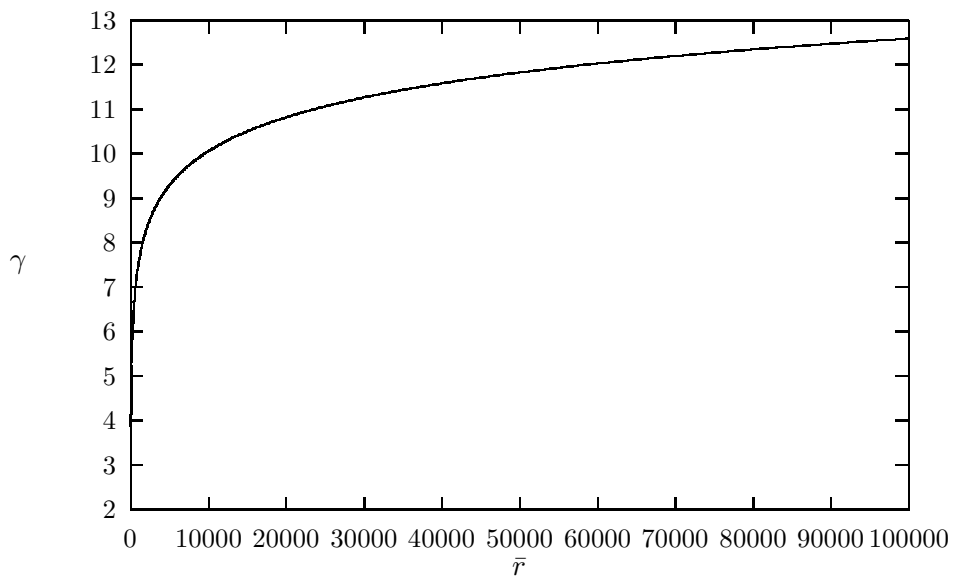


Figure 11: Behaviour of the Lorentz factor γ for co-rotating and counter-rotating orbits with a linearly rising degree of ionization: $\bar{C} = 1.1\bar{r}$; distance scale enlarged to the first parsec from the centre .

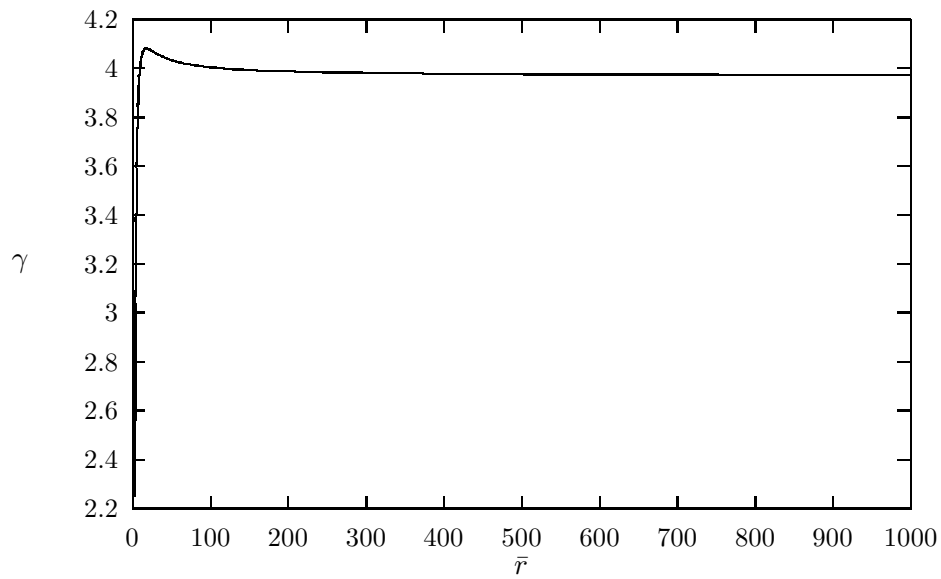


Figure 12: Behaviour of the Lorentz factor γ for co-rotating and counter-rotating orbits under the effect of the pressure gradients. $\bar{\mathcal{D}} = 5$, $\Gamma_i = 0.1$, $\theta_i = \pi/4$.

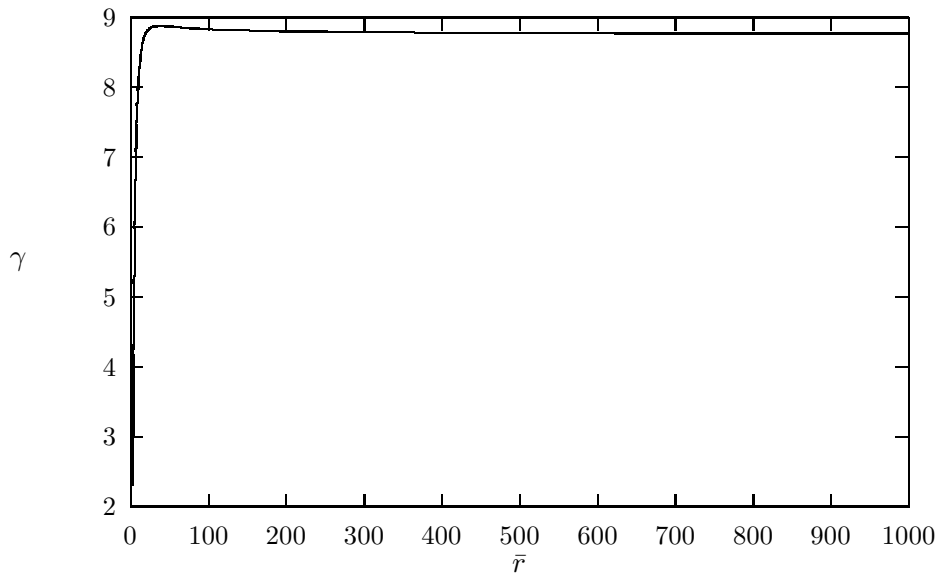


Figure 13: Behaviour of the Lorentz factor γ for co-rotating and counter-rotating orbits under the effect of the pressure gradients. $\bar{\mathcal{D}} = 10$, $\Gamma_i = 0.1$, $\theta_i = \pi/4$.

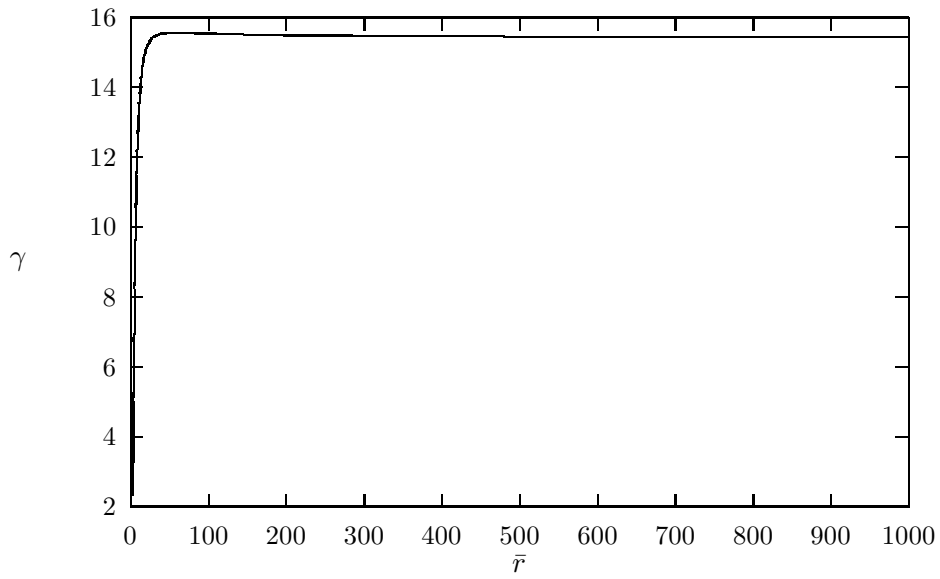


Figure 14: Behaviour of the Lorentz factor γ for co-rotating and counter-rotating orbits under the effect of the pressure gradients. $\bar{\mathcal{D}} = 15$, $\Gamma_i = 0.1$, $\theta_i = \pi/4$.

References

- [1] Sikora, M. et al., 1996, MNRAS, 280, 781-796
- [2] de Felice, F., Carlotto, L., 1997, Ap.J., 481, 116-126
- [3] Karas, V., Dovciak, M., 1997, General Relativity and Gravitation, Vol. 29, No. 0
- [4] de Felice, F., 1980, J. Phys. A: Math. Gen., 13:1701-1708
- [5] Williams Reva K., 1995, Phys. Rev., vol 51, n 10, 5387-5427
- [6] Begelman, M.C., Blandford, R.D., Rees, M.J., 1984, Rev. Mod. Phys., vol 56, No 2, Part I
- [7] Ghisellini et al., 1993, Ap.J., 407: 65-82
- [8] de Felice, F. and Preti G., 1998, Class. Quantum Grav. 16, 2929-2935
- [9] O'Neil B. 1995 *The Geometry of Kerr Black Holes*, A.K. Peters
- [10] Unwin, S.C., Cohen, M. H., 1989, Ap. J., 340: 117-128